Chinese Journal of Electronics
Vol.23, No.3, July 2014

Efficient Two-Dimensional Extrapolation Technique of Scattering Problems Involving Dielectric Objects Using PMCHWT Formulation*

LV Zhengliang, GONG Shuxi, ZHANG Pengfei and HONG Tao

(*Key Laboratory of Antennas and Microwave Technology, Xidian University, Xi'an 710071, China*)

Abstract — An efficient extrapolation technique of Radar cross-section (RCS) combines with Poggio-Miller-Chang-Harrington-Wu-Tsai (PMCHWT) formulation is presented for the fast analysis by arbitrary shaped three-dimensional homogeneous lossy dielectric objects. The PMCHWT formulation obtained in a well-known manner is discretized to matrix equations using the Method of moments (MoM). For the RCS is highly angular dependent as well as frequency, a novel rational function scheme is extended to the induced currents associated with PMCHWT, which can provide fast and accurate radar cross-section computation in both the frequency domain and spatial domain simultaneously. Numerical results are presented for two canonical dielectric scatterers.

Key words — Radar cross-section, Poggio-Miller-Chang-Harrington-Wu-Tsai (PMCHWT) formulation, Extrapolation technique, Dielectric objects.

I. Introduction

Much attention has been given to the analysis of scattering properties for dielectric objects under the excitation of electromagnetic waves in the Computational electromagnetics (CEM) community[1]. Among various surface integral formulations for electromagnetic interactions with homogeneous material bodies studied, PMCHWT formulation is one of the most widely used approach[2]. For most complex case of dielectric scattering, PMCHWT formulation is known to be stable and provide accurate results. As compared with the traditional Volume integral equation (VIE) method, the PMCHWT method generally requires smaller number of unknowns for scattering problems involving dielectric objects[3,4]. Furthermore, it has also been realized that once dielectric object with high permittivity is involved, the convergence rate in PMCHWT will be much faster than the VIE method. A complete comparison has yet to be presented for the Müller formulation in literature, upon discretization, the Müller integral equation yields numerical solutions that are far less accurate than those obtained by discretizing the PMCHWT integral equation on the same mesh[5].

The recent development and extension of the PMCHWT formulations is overcoming its drawback. Generalization for objects made of multiple dielectric regions and mixed metallic, some hybrid formulations based on the PMCHWT formulations are employed to analyze the scatterings, such as EFIE-PMCHWT, JMCFIE[6,7]. The Calderón preconditioned PMCHWT integral equation is also introduced to cure the dense discretization breakdown[8−10]. In Ref.[11], a brief discussion on the resonance problem of the PMCHWT formulations associated with finite microstrip structures is presented.

However, to obtain the RCS in both the frequency domain and spatial domain simultaneously using the PMCHWT, one has to repeat the calculation at each frequency point and angular point. In many practical applications, the recently progress focuses on the construction of "fast" methods to predict the monostatic RCS of a target. In Ref.[12], the author enumerated the two-dimensional problems faced currently and introduced several important algorithms and the applications. Some efficient techniques, such as Asymptotic waveform evaluation (AWE) technique[13], the impedance matrix interpolation technique and the Cauchy method have been successfully applied to the extrapolation of the RCS alone versus frequency or angular curves in appearing documents. Among these techniques, the Maehly approximation in Ref. [14] is more easily applicable in conjunction with PMCHWT, providing high accuracy and efficiency for dielectric objects scattering problems.

In this paper, a simple and an efficient modeling scheme is presented to deal with scattering problems involving dielectric objects. Moreover, one promising approach combines with the PMCHWT to speed up the impendence matrix solving. In this optimization, the Chebyshev series is matched to be a rational function via Maehly approximation to improve the accuracy. As a result, we attempt to expand the Maehly approximation to include multidimensional extrapolation technique. Finally, several numerical results are included to illustrate the validness.

*Manuscript Received Mar. 2013; Accepted Oct. 2013. This work is supported by the National Natural Science Foundation of China (No.61201018), the Fundamental Research Funds for the Center Universities (No.K5051202010) and Specialized Research Fund for the Doctoral Program of Higher Education (No.20120203120011).

II. Theory

1. A brief overview of SIE involving homogeneous dielectric objects

Arbitrarily shaped homogeneous dielectric objects can be analyzed based on the model shown in Fig. 1. The original model is decomposed into an interior region, defined by permittivity ε_1 and permeability μ_1, and into an exterior region, defined by permittivity ε_2 and permeability μ_2. The scatterer with an incident plane wave $(\boldsymbol{E}^i, \boldsymbol{H}^i)$ is located in region 2 free space medium. $\boldsymbol{n}_1$ stands for the outward pointing unit normal vector.

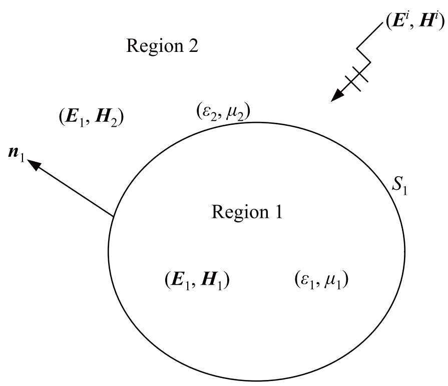

Fig. 1. Geometry of a homogeneous lossy dielectric scatterer in free space medium

According to Love's equivalence principle, the solution can be formulated in terms of an equivalent surface electric current and an equivalent surface magnetic current as follow

$$\boldsymbol{E}_1 = j\omega \boldsymbol{A}_1\left(\boldsymbol{J}_1(k,\theta)\right) + \nabla\phi_1\left(\boldsymbol{J}_1(k,\theta)\right) + \frac{1}{\varepsilon_1}\nabla\times\boldsymbol{F}_1\left(\boldsymbol{M}_1(k,\theta)\right) \quad \text{(for } \boldsymbol{r} \text{ on or inside S1)} \tag{1}$$

$$\boldsymbol{H}_1 = j\omega \boldsymbol{F}_1\left(\boldsymbol{M}_1(k,\theta)\right) + \nabla\varphi_1\left(\boldsymbol{M}_1(k,\theta)\right) - \frac{1}{\mu_1}\nabla\times\boldsymbol{A}_1\left(\boldsymbol{J}_1(k,\theta)\right) \quad \text{(for } \boldsymbol{r} \text{ on or inside S1)} \tag{2}$$

$$\boldsymbol{E}_2^s = -j\omega \boldsymbol{A}_2\left(\boldsymbol{J}_1(k,\theta)\right) - \nabla\phi_2\left(\boldsymbol{J}_1(k,\theta)\right) - \frac{1}{\varepsilon_2}\nabla\times\boldsymbol{F}_2\left(\boldsymbol{M}_1(k,\theta)\right) \quad \text{(for } \boldsymbol{r} \text{ on or outside S1)} \tag{3}$$

$$\boldsymbol{H}_2^s = -j\omega \boldsymbol{F}_2\left(\boldsymbol{M}_1(k,\theta)\right) - \nabla\varphi_2\left(\boldsymbol{M}_1(k,\theta)\right) + \frac{1}{\mu_2}\nabla\times\boldsymbol{A}_2\left(\boldsymbol{J}_1(k,\theta)\right) \quad \text{(for } \boldsymbol{r} \text{ on or outside S1)} \tag{4}$$

where the various vector potentials $\boldsymbol{A}_h(k,\theta)$ and $\boldsymbol{F}_h(k,\theta)$ and the scalar potentials $\phi_h(k,\theta)$ and $\varphi_h(k,\theta)$, for $h = 1$ or $h = 2$ are given by

$$\boldsymbol{A}_h\left(\boldsymbol{X}(k,\theta)\right) = \mu_h \int_S \boldsymbol{X}\left(\boldsymbol{r}';k,\theta\right) g_h\left(\boldsymbol{r},\boldsymbol{r}';k\right) ds' \tag{5}$$

$$\boldsymbol{F}_h\left(\boldsymbol{X}(k,\theta)\right) = \varepsilon_h \int_S \boldsymbol{X}\left(\boldsymbol{r}';k,\theta\right) g_h\left(\boldsymbol{r},\boldsymbol{r}';k\right) ds' \tag{6}$$

$$\phi_h\left(\boldsymbol{X}(k,\theta)\right) = \frac{j}{\omega\varepsilon_h}\int_S \nabla'\cdot\boldsymbol{X}\left(\boldsymbol{r}';k,\theta\right) g_h\left(\boldsymbol{r},\boldsymbol{r}';k\right) ds' \tag{7}$$

$$\varphi_h\left(\boldsymbol{X}(k,\theta)\right) = \frac{j}{\omega\mu_h}\int_S \nabla'\cdot\boldsymbol{X}\left(\boldsymbol{r}';k,\theta\right) g_h\left(\boldsymbol{r},\boldsymbol{r}';k\right) ds' \tag{8}$$

In obtaining the above expressions, S denotes the surface. The vectors $\boldsymbol{r}$ and $\boldsymbol{r}'$ are position vectors to observation and source points, respectively, from a global coordinate origin. The Green's function defined in Eqs.(5)–(8) for $h = 1, 2$ is given by

$$g_h\left(\boldsymbol{r},\boldsymbol{r}';k\right) = \frac{e^{-jk_hR}}{4\pi R} \tag{9}$$

$$R = \left|\boldsymbol{r}-\boldsymbol{r}'\right| \tag{10}$$

And the propagation constant is

$$k_h = \omega\sqrt{\mu_h\varepsilon_h} \tag{11}$$

On enforcing the boundary condition, the following combined field integral equations are obtained in terms of the unknown surface equivalent electric and magnetic currents:

$$\Big[L_1\Big(\boldsymbol{J}_1(k,\theta)\Big) + L_2\left(\boldsymbol{J}_1(k,\theta)\right) + K_1\left(\boldsymbol{M}_1(k,\theta)\right) + K_2\left(\boldsymbol{M}_1(k,\theta)\right)\Big]_{\tan} = -\boldsymbol{E}^i\Big|_{\tan} \tag{12}$$

$$\Big[-K_1\Big(\boldsymbol{J}_1(k,\theta)\Big) - K_2\left(\boldsymbol{J}_1(k,\theta)\right) + \frac{L_1\left(\boldsymbol{M}_1(k,\theta)\right)}{\eta_1^2} + \frac{L_2\left(\boldsymbol{M}_1(k,\theta)\right)}{\eta_2^2}\Big]_{\tan} = -\boldsymbol{H}^i\Big|_{\tan} \tag{13}$$

where the subscript "tan" stands for the tangential component, the operators $L_h$and K_h are given by:

$$L_h\left(\boldsymbol{X}(k,\theta)\right) = -j\omega\boldsymbol{A}_h\left(\boldsymbol{X}(k,\theta)\right) - \nabla\phi_h\left(\boldsymbol{X}(k,\theta)\right) \tag{14}$$

$$\begin{aligned} K_h\left(\boldsymbol{X}(k,\theta)\right) &= \int_S \boldsymbol{X}\left(\boldsymbol{r}';k,\theta\right)\times\nabla g_h\left(\boldsymbol{r},\boldsymbol{r}';k\right) ds' \\ &= \boldsymbol{n}\times\frac{\boldsymbol{X}\left(\boldsymbol{r}';k,\theta\right)}{2} + P.V.\int_S \boldsymbol{X}\left(\boldsymbol{r}';k,\theta\right)\times\nabla g_h\left(\boldsymbol{r},\boldsymbol{r}';k\right) ds' \\ &= \boldsymbol{n}\times\frac{\boldsymbol{X}\left(\boldsymbol{r}';k,\theta\right)}{2} + K_h\left(\boldsymbol{X}(k,\theta)\right) \end{aligned} \tag{15}$$

In Eq.(15), $P.\ V.$ stands for the Cauchy principal value integration. To solve Eqs.(14) and (15) using MoM, two sets of basis functions are used to discretize the surface electric current and surface magnetic current, respectively. Let N represents the total number of edges, then

$$\boldsymbol{M}_1(k,\theta) = \eta_0\sum_{n=1}^{N} P_n\boldsymbol{f}_n \tag{16}$$

$$\boldsymbol{J}_1(k,\theta) \cong \sum_{n=1}^{N} I_n\boldsymbol{f}_n \tag{17}$$

where $\boldsymbol{f}_n$ denotes Rao-Wilton-Glisson (RWG) basis function. Eqs.(16) and (17) can be transformed into a matrix equation using $\boldsymbol{f}_m$ as testing functions

$$\begin{bmatrix} \boldsymbol{\alpha}_1(k,\theta)+\boldsymbol{\alpha}_2(k,\theta) & \boldsymbol{\beta}_1(k,\theta)+\boldsymbol{\beta}_2(k,\theta) \\ -\boldsymbol{\beta}_1(k,\theta)-\boldsymbol{\beta}_2(k,\theta) & \dfrac{\varepsilon_{1r}}{\mu_{1r}}\boldsymbol{\alpha}_1(k,\theta)+\dfrac{\varepsilon_{2r}}{\mu_{2r}}\boldsymbol{\alpha}_2(k,\theta) \end{bmatrix} \cdot \begin{bmatrix} \boldsymbol{I} \\ \boldsymbol{P} \end{bmatrix} = \begin{bmatrix} \boldsymbol{V}(k,\theta) \\ \boldsymbol{U}(k,\theta) \end{bmatrix} \tag{18}$$

where

$$\boldsymbol{\alpha}_h^{mn}(k,\theta) = <\boldsymbol{f}_m, L_h\left(\boldsymbol{f_n}\right)> \tag{19}$$

$$\boldsymbol{\beta}_h^{mn}(k,\theta) = \eta_0 <\boldsymbol{f}_m, K_h\left(\boldsymbol{f_n}\right)> \tag{20}$$

$$\boldsymbol{V}^m(k,\theta) = \ <\boldsymbol{f}_m, -\boldsymbol{E}^i> \tag{21}$$

$$\boldsymbol{U}^m(k,\theta) = \eta_0 <\boldsymbol{f}_m, -\boldsymbol{H}^i> \tag{22}$$

The expression $< \cdot, \cdot >$ stands for the inner product. The number of unknowns in the equation is $2N$.

2. Two-Dimensional extrapolation technique

For the RCS over a desired frequency and angular range, the induced currents are expanded by the bivariate Chebyshev series, which can be used as well as the best polynomial approximation. To represent the data in question efficiently, it is better achieved by casting the coefficients of Chebyshev series *via* the Maehly approximation into a rational function. For the specific frequency domain $k \in [k_a, k_b]$ and angular domain $\theta \in [\theta_a, \theta_b]$, the coordinate transform is used as

$$\begin{cases} k = \frac{1}{2}[\tilde{k}(k_b - k_a) + (k_b + k_a)], \quad \tilde{k} \in [-1, 1] \\ \theta = \frac{1}{2}[\tilde{\theta}(\theta_b - \theta_a) + (\theta_b + \theta_a)], \quad \tilde{\theta} \in [-1, 1] \end{cases} \tag{23}$$

$$I_n(k, \theta) \approx \sum_{i=0}^{N_1} \sum_{j=0}^{N_2} c_n^{i,j} T_i(\tilde{k}) T_j(\tilde{\theta}) \tag{24}$$

where

$$c_n^{i,j} = \frac{d_i d_j}{(N_1 + 1)(N_2 + 1)} \sum_{p=0}^{N_1} \sum_{q=0}^{N_2} I_n(k_p, \theta_q) T_i(\tilde{k}_p) T_j(\tilde{\theta}_q) \tag{25}$$

d_0 is set to be 1 in common and $d_i = d_j = 2$ for $i = 1, ..., N_1, j = 1, ..., N_2$. $\tilde{k}_p$ and $\tilde{\theta}_q$ are the Chebyshev zeroes for $T_{N_1+1}(\tilde{k})$ and $T_{N_2+1}(\tilde{\theta})$, respectively. $k_p \in [k_a, k_b]$ and $\theta_q \in [\theta_a, \theta_b]$ can be obtained use the Eq.(23). $c_n^{i,j}$ denotes the Chebyshev coefficients. To improve the accuracy of the numerical solution, the improved Maehly approximation for each $I_n(k, \theta)$ is

$$\begin{aligned} I_n(k,\theta) &\approx \frac{\sum_{p=0}^{L_k} \sum_{q=0}^{L_\theta} a_n^{p,q} T_p(\tilde{k}) T_q(\tilde{\theta})}{\sum_{k=0}^{M_k} \sum_{r=0}^{M_\theta} b_n^{k,r} T_k(\tilde{k}) T_r(\tilde{\theta})} \\ &= \frac{a_n^{0,0} T_0(\tilde{k}) T_0(\tilde{\theta}) + \cdots + a_n^{L_k, L_\theta} T_{L_k}(\tilde{k}) T_{L_\theta}(\tilde{\theta})}{b_n^{0,0} T_0(\tilde{k}) T_0(\tilde{\theta}) + \cdots + b_n^{M_k, M_\theta} T_{M_k}(\tilde{k}) T_{M_\theta}(\tilde{\theta})} \end{aligned} \tag{26}$$

where the integers (L_k, L_θ),(M_k, M_θ) are the orders of the zero and pole expansions of the Maehly rational function respectively. Substitute Eq.(26) into (24) and use the Eq.(27)

$$T_p(x) T_q(x) = \frac{1}{2}(T_{p+q}(x) + T_{|p-q|}(x)) \tag{27}$$

$T_n(x)$ stands for the fundamental recurrence relation of the Chebyshev polynomial with the initial conditions $T_0(x) = 1, T_0(x) = x$.

$$T_{n+1}(x) = 2x T_n(x) - T_{n-1}(x) \tag{28}$$

The coefficients $a_n^{p,q}$ and $b_n^{k,r}$ are then found from the following Eqs.(29) and (30). Once the coefficients of the rational function are calculated, the induced currents distribution can be obtained at any frequency and angle point within the whole frequency and angular range.

$$\begin{aligned} &\frac{1}{2}\sum_{r=1}^{M_\theta} b_n^{0,r}(c_n^{0,L_\theta+s+r} + c_n^{0,L_\theta+s-r}) + \frac{1}{2}\sum_{k=1}^{M_k} b_n^{k,0} c_n^{k,L_\theta+s} \\ &\qquad + \frac{1}{4}\sum_{k=1}^{M_k}\sum_{r=1}^{M_\theta} b_n^{k,r}(c_n^{k,L_\theta+s+r} + c_n^{k,L_\theta+s-r}) = -c_n^{0,L_\theta+s} \\ &\frac{1}{2}\sum_{r=1}^{M_\theta} b_n^{0,r} c_n^{L_k+l,r} + \frac{1}{2}\sum_{k=1}^{M_k} b_n^{k,0}(c_n^{L_k+l+k,0} + c_n^{L_k+l-k,0}) \\ &\qquad + \frac{1}{4}\sum_{k=1}^{M_k}\sum_{r=1}^{M_\theta} b_n^{k,r}(c_n^{L_k+l+k,r} + c_n^{L_k+l-k,r}) = -c_n^{L_k+l,0} \\ &\frac{1}{2}\sum_{r=1}^{M_\theta} b_n^{0,r}(c_n^{L_k+l,L_\theta+s+r} + c_n^{L_k+l,L_\theta+s-r}) \\ &\qquad + \frac{1}{2}\sum_{k=1}^{M_k} b_n^{k,0}(c_n^{L_k+l+k,L_\theta+s} + c_n^{L_k+l-k,L_\theta+s}) \\ &\qquad + \frac{1}{4}\sum_{k=1}^{M_k}\sum_{r=1}^{M_\theta} b_n^{k,r}(c_n^{L_k+l+k,L_\theta+s+r} + c_n^{L_k+l+k,L_\theta+s-r}) \\ &\qquad + \frac{1}{4}\sum_{k=1}^{M_k}\sum_{r=1}^{M_\theta} b_n^{k,r}(c_n^{L_k+l-k,L_\theta+s+r} + c_n^{L_k+l-k,L_\theta+s-r}) \\ &\qquad = -c_n^{L_k+l,L_\theta+s} \end{aligned} \tag{29}$$

where $l = 1, ..., M_k,\ s = 1, ..., M_\theta$.

$$\begin{aligned} a_n^{0,0} &= c_n^{0,0} + \frac{1}{2}\sum_{r=1}^{M_\theta} b_n^{0,r}(c_n^{0,r} + c_n^{0,r}) + \frac{1}{2}\sum_{k=1}^{M_k} b_n^{k,0} c_n^{k,0} \\ &\quad + \frac{1}{4}\sum_{k=1}^{M_k}\sum_{r=1}^{M_\theta} b_n^{k,r} c_n^{k,r} \\ a_n^{0,q} &= c_n^{0,q} + \frac{1}{2}\sum_{r=1}^{M_\theta} b_n^{0,r}(c_n^{0,q+r} + c_n^{0,|q-r|}) + \frac{1}{2}\sum_{k=1}^{M_k} b_n^{k,0} c_n^{k,q} \\ &\quad + \frac{1}{4}\sum_{k=1}^{M_k}\sum_{r=1}^{M_\theta} b_n^{k,r}(c_n^{k,q+r} c_n^{k,|q-r|}) \\ &\quad + \frac{1}{4}\sum_{k=1}^{M_k} b_n^{k,q} c_n^{k,q} + \frac{1}{2} b_n^{0,q} c_n^{0,0} \\ a_n^{p,0} &= c_n^{p,0} + \frac{1}{2}\sum_{r=1}^{M_\theta} b_n^{0,r} c_n^{p,r} + \frac{1}{2}\sum_{k=1}^{M_k} b_n^{k,0}(c_n^{|p-k|,0} + c_n^{p+k,0}) \\ &\quad + \frac{1}{4}\sum_{k=1}^{M_k}\sum_{r=1}^{M_\theta} b_n^{k,r}(c_n^{|p-k|,r} + c_n^{p+k,r}) \\ &\quad + \frac{1}{4}\sum_{r=1}^{M_\theta} b_n^{p,r} c_n^{0,r} + \frac{1}{2} b_n^{p,o} c_n^{0,0} \\ a_n^{p,q} &= c_n^{p,q} + \frac{1}{2}\sum_{r=1}^{M_\theta} b_n^{0,r}(c_n^{p,q+r} c_n^{p,|q-r|}) + \frac{1}{2}\sum_{k=1}^{M_k} b_n^{k,0}(c_n^{|p-k|,q} + c_n^{p+k,q}) \\ &\quad + \frac{1}{4}\sum_{k=1}^{M_k}\sum_{r=1}^{M_\theta} b_n^{k,r}(c_n^{|p-k|,q+r} + c_n^{|p-k|,|q-r|} \\ &\quad + c_n^{p+k,q+r} + c_n^{p+k,|q-r|}) + \frac{1}{4}\sum_{k=1}^{M_k} b_n^{k,q}(c_n^{|p-k|,0} + c_n^{p+k,0}) \\ &\quad + \frac{1}{4}\sum_{r=1}^{M_\theta} b_n^{p,r}(c_n^{0,q+r} + c_n^{0,|q-r|}) \\ &\quad + \frac{1}{2} b_n^{0,q} c_n^{p,0} + \frac{1}{2} b_n^{p,0} c_n^{0,q} + \frac{1}{4} b_n^{p,q} c_n^{0,0} \end{aligned} \tag{30}$$

where $p = 1, ..., L_k,\ q = 1, ..., L_\theta$.

III. Results

In this section, some numerical results corroborate the accuracy and efficiency of the newly implemented Maehly approximation combined with PMCHWT for obtaining 3-D RCS pattern. All the computations were carried out on a Pentium 2.99GHz PC.

The first example is a combined object located in free space. The object consists of a cube $(0.5\lambda \times 0.5\lambda \times 0.5\lambda)$ and a sphere of radius 0.25λ with a ϕ-polarized plane wave incident.

The relative dielectric constant of the model is $\varepsilon_r = 4$. The 1/4 part of the sphere is embedded in the cube. The combined model is discretized with 468 triangular patches resulting into 702 basis functions. Fig.2(a) clearly shows the monostatic RCS *versus* frequency obtained by both the directly calculated and Maehly approximation. The proposed method can acquire high accuracy compared with MoM. Fig.2 (b) shows the monostatic RCS of the combined object versus θ from $-90°$ to $90°$ at $\phi = 30°$, $45°$and $90°$. The results obtained by the direct MoM are plotted for comparison. This comparison in order to show Maehly approximation can produce an accurate solution with 0.5° increments at a different incident angle. It is obvious that the full line and the line with symbol are indistinguishable in Fig.2 (b). Fig.3 shows the 3-D RCS pattern (dependent on both θ and f) of the combined object obtained by Maehly approximation ($L_\theta = 8, M_\theta = 8, L_k = 8, M_k = 8$) . The CPU time required for MoM and two dimensional Maehly approximation are 1812 and 167 min, by contrast, the proposed method is superior in terms of the CPU time to predict 3-D monostatic RCS pattern.

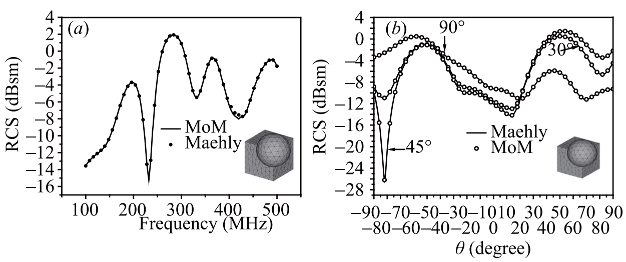

Fig. 2. Monostatic RCS of the first model. (a) RCS *versus* frequency. (b) RCS *versus* angle

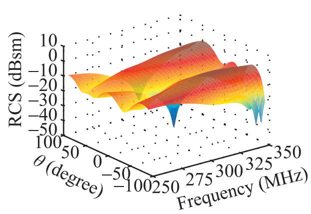

Fig. 3. 3-D RCS pattern of the first model simultaneous *versus* frequency and angle

The second example considered in this paper consists of a cone (Rb=1m, h=2m) and a parabolic body (radius =1m, focal depth=0.5m). The combined object excited by a ϕ-polarized plane wave at ϕ=0 . Meanwhile, the AWE technique with the Padé approximation based on the PMCHWT is introduced to these comparisons. The relative dielectric constant of the case is $\varepsilon_r = 4$. There are 834 flat triangles used to discretize the object resulting into 1251 unknowns. Fig.4 shows the monostatic RCS of the combined object *versus* angle (f_0=300MHz) obtained by MoM, AWE technique and Maehly approximation, respectively. In this comparison, the MoM results agree well with the Maehly results. On the other hand, although AWE can usually achieve efficient wide response analysis, the large number of unknowns in the algorithm causes more memory requirements than Maehly. The 3-D RCS pattern of the combined object simultaneous *versus* angle and frequency obtained by Maehly approximation is shown in Fig.5. According to the experienced formula, it can be also noted that the rational function has the smallest error in the whole frequency domains and angular domains when $L = M$ or $L = |M - 1|$, and the curves representing the Maehly approximation and MoM almost coincide. For the calculation time, the proposed method took 194min CPU time for calculation of the RCS frequency and angular responses with 10MHz frequency and 3° angular increments, approximately 1/6 of the CPU time used by the MoM.

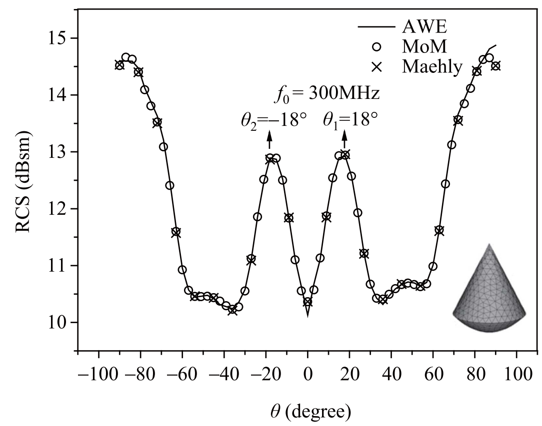

Fig. 4. Monostatic RCS of the combined object *versus* θ

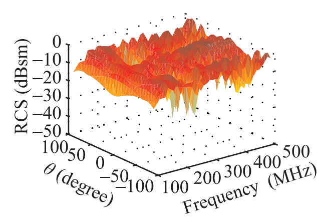

Fig. 5. 3-D RCS pattern of the combined object simultaneous versus frequency and angle

IV. Error Discussion

For the application of the proposed method to a specific problem, it is apparently critical to choose the appropriate number of Chebyshev nodes *via* Maehly approximation to cover the entire band. A simplified error function is reformed from Ref.[14]. The relative root mean square (RMS) RCS error of a specific object is calculated by

$$Err_{RMS} = \left\{ \frac{1}{N \times M} \sum_{j=1}^{N \times M} \left| 10 \log_{10} \left(\frac{\tilde{\sigma}(k,\theta)_j}{\sigma(k,\theta)_j} \right) \right|^2 \right\}^{1/2} \tag{31}$$

Where sampling point $(k,\theta)_j$ $(j = 1, 2, \ldots, N \times M)$ is selected from the relevant N frequency points and M angular points, while $\tilde{\sigma}(k,\theta)_j$ and $\sigma(k,\theta)_j$ are the RCS obtained by the proposed method and the direct solution method, respectively. Fig.6 is demonstrated the relative RMS RCS error of the above models vary with the respective value of order$n(L = M = n)$.

V. Conclusion

In this paper, the monostatic RCS pattern in both a broad frequency domain and spatial domain simultaneously calculation by the 2-D extrapolation technique combined with PMC-

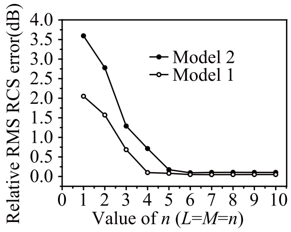

Fig. 6. The relative RMS RCS error of the two models vary with the respective value of n

HWT is generated. It was observed that the proposed method is especially appropriate for the fast and accurate 3-D monostatic RCS pattern. Although only simple dielectric scatterers are taken into account in this paper, the present numerical results show that the newly method is accurate and efficient. The accuracy of the proposed two-dimensional approximation approach and its relation to the order of the best polynomial series is preliminary in overall consideration.

References

[1] J. R. Mautz and R. F. Harrington, "Boundary formulation for aperturecoupling problems", *International Journal of Electronics and Communications*, Vol.34, pp.377–384, 1980.

[2] T. W. Lloyd, J. M. Song, G. Kang, and C. C. Lu, "Numerical study of surface integral formulations for homogeneous bodies", *Proc. IEEE Antennas and Propagation Society Int. Symp.*, Monterey, California. Vol.4, pp.3895–3898, 2004.

[3] I. T. Chiang and W. C. Chew, "A coupled PEC-TDS surface integral equation approach for electromagnetic scattering and radiation from composite metallic and thin dielectric objects", *IEEE. Trans. Antennas Propag.*, Vol.54, No.11, pp.3511–3516, 2006.

[4] Y. Chen, S. Yang, S. He, and Z. Nie, "Fast analysis of microstrip antennas over a frequency band using an accurate MoM matrix interpolation technique", *Progress in Electromagnetics Research*, Vol.109, pp.301–324, 2010.

[5] P. Ylä-Oijala and M. Taskinen, "Well-conditioned Muller formulation for electromagnetic scattering by dielectric objects", *IEEE Trans. Antennas Propagat.*, Vol.53, No.10, pp.3316–3323, 2005.

[6] P. Ylä-Oijala and M. Taskinen, "Application of combined field integral equation for electromagnetic scattering by composite metallic and dielectric objects", *IEEE Trans. Antennas Propagat.*, Vol.53, No.3, pp.1168–1173, 2005.

[7] H. Contopanagos , B. Dembart , M. Epton , J. J. Ottusch, V. Rokhlin, J. L. Visher and S. M. Wandzura, "Well-conditioned boundary integral equations for three-dimensional electromagnetic scattering", *IEEE Trans. Antennas Propag.*, Vol.50, No.12, pp.1824–1830, 2002.

[8] Olyslager, F., Cools, K., Peeters, J., Andriulli, F.P., Michielssen, E., "A Calderon multiplicative preconditioner for the PMCHWT integral equation", *Antennas and Propagation Society International Symposium*, APSURSI '09, IEEE, pp.1–4, 2009.

[9] Beghein, Y., Cools, K., Andriulli, F.P., De Zutter, D., Michielssen, E., "A Calderon multiplicative preconditioner for the PMCHWT equation for scattering by chiral objects", *IEEE Transactions on Antennas and Propagation*, Vol.60, No.9, pp.4239–4248, 2012.

[10] Cools, K., Andriulli, F.P., Michielssen, E., "A Calderon multiplicative preconditioner for the PMCHWT integral equation", *IEEE Transactions on Antennas and Propagation*, Vol.59, No.12, pp.4579–4587, 2011.

[11] W. J. Zhao , L. W. Li and K. Xiao, "Analysis of electromagnetic scattering and radiation from finite microstrip structures using an EFIE-PMCHWT formulation", *IEEE Trans. Antennas Propag.*, Vol.58, No.7, NO.7, pp.2468–2473, 2010.

[12] XIONG Ye, FANG Da-gang, LIU Tie-jun "Interpolation and extrapolation in computational electromangnetics", *Chinese Journal of Radio Science*, Vol.17, No.4, pp.325–330, 2002.

[13] C. M. Tong, W. Hong, N. C. Yuan, "Simultaneous extrapolation of RCS in both angular and frequency domains based on AWE technique", *Microwave and Optical Technology Letters.*, Vol.32, No.4, pp.290–293, 2002.

[14] M. S. Chen, X. L. Wu, W. Sha, and Z. X. Huang, "Fast and accurate radar cross-section computation over a broad frequency band using the best uniform rational approximation", *IET Microw. Antennas Propag.*,Vol.2, No.2, pp.200–204, 2008.

LV Zhengliang was born in Zhejiang Province, China, in 1986. He received the B.S. and M.S. degrees in electronic engineering from Xidian University, Xi'an, China, in 2008 and 2010, respectively where he is currently working toward the Ph.D. degree in electromagnetic field and microwave technology. His research interests include computational electromagnetic, fast algorithms for electromagnetic scattering and radiation, hybrid methods, and EMC analysis.

GONG Shuxi received the B.S. and M.S. degrees from Xidian University, Xi'an, China, in 1982 and 1984, respectively, and the Ph.D. degree from Xi'an Jiao Tong University, Xi'an, China, in 1988. He is currently a full professor and director of the National Key Laboratory of Science and Technology on Antennas and Microwaves. His research interests include antenna theory and technology, prediction and control of antenna RCS, and RCS calculation of complex targets. He has authored or co-authored over 200 refereed journal papers. He has also authored *Principles of Generalized Eigenfunction Expansions in Electromagnetic Theory* (Xi'an: Xidian University Press, 2010), *Prediction and Reduction of Antenna Radar Cross Section* (Xi'an: Xidian University Press, 2010), and *Antennas for Mobile Communication Systems* (Beijing: Electronics Industry Press, 2011).

ZHANG Pengfei received the B.E., M.E. and Ph.D. degrees in electronic engineering from Xidian University, Xi'an, China, in 2001, 2006, and 2008, respectively. Since 2006, he has joined the Department of Electrical Engineering of Xidian University. He is currently an associate professor at the National Key Laboratory of Antennas and Microwave Technology, Xidian University. His research interests include the stealth technology of antenna, analytical and computational electromagnetic.

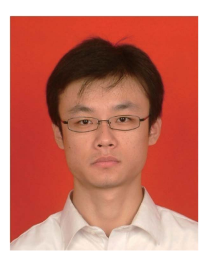

HONG Tao was born in Shaanxi Province, in 1983. He received the Ph. D. degree in electromagnetic and microwave technology from Xidian University in 2011. Currently he is an associate professor in School of Electronic Engineering of Xidian University. His research interests include electromagnetic scattering theory, computational electromagnetics and antenna scattering.